Eur Biophys J (1997) 25: 311–317

ARTICLE

A. C. Clewlow · N. Errington · A. J. Rowe

Analysis of data captured by an on-line image capture system from an analytical ultracentrifuge using schlieren optics

Received: 1 November 1996 / Accepted: 15 January 1997

Abstract The recent development in this laboratory of an automated data capture system, for refractometric optics on the analytical ultracentrifuge has removed the requirement for tedious and time consuming manual acquisition which had led to a decline in the use of schlieren optics. At the same time this system has increased the amount of data easily available from such an optical system with maintained or increased precision. From the advent of such a system has arisen the need for a package to facilitate the analysis of these data and to extend the range of analytical methods used. Using the improved data sets now available has also enabled us to successfully use methods which have lapsed in popularity over the last two decades. We have also been able to successfully apply radial derivative methods (Bridgman 1942) which have not routinely been applied to the analysis of sedimentation velocity experiments using schlieren optics. In this paper we describe the methods we have so far used to analyse data and present results for previously well defined molecules to demonstrate that the results obtained are reliable.

Key words Analytical ultracentrifuge · Schlieren optics · Molecular weight · Sedimentation coefficient · On-line data analysis

Introduction

The aim of this paper is to demonstrate the analysis of captured schlieren optical images to provide molecular weight and sedimentation coefficient data. The optical system developed will not be described in detail. The three main optical systems used in analytical ultracentrifuges (AUCs) are absorption, Rayleigh interference and differential refractometric (schlieren) optics. In our laboratory we have developed an on-line image capture system capable of being used with all three optical systems. For reasons detailed later we have concentrated upon the analysis of images from the schlieren optical system.

Traditionally data from schlieren optical systems on the analytical ultracentrifuge have been captured using tedious and time consuming microcomparator methods (e.g. Schachman 1959). The development of the on-line data capture system means that this is no longer the case and data from schlieren optical images can be captured much more quickly and in greater detail than was previously possible without large expenditures of time.

A. C. Clewlow · N. Errington · A. J. Rowe (✉)
NCMH, Department of Biochemistry, University of Leicester, University Road, Leicester LE1 7RH, UK
(Fax:+44 (116) 252 5260; email: AJR@le.ac.uk)

Instrumentation and software

Our system uses a cooled CCD camera (768×512 pixels, Photonic Science, with NIH-Image software) to capture series of images. This image capture system was mounted on an MSE MkII analytical ultracentrifuge (MSE Instruments, Crawley, UK). In-house macros written for NIH-Image capture pixel profiles of the image in a radial direction which are then processed using our PASCAL algorithm LINEDEF to give the line from the schlieren image to better than pixel resolution. These data are then converted into dn/dr (in pixel values) versus radial distance (cm) using pre-defined reference points on the image.

LINEDEF is the major component in this system. Schlieren images contain lines whose thickness may vary considerably and so conventional line-following algorithms may not be stable enough to cope with these images when run repeatedly. LINEDEF has proven itself able to comply with these criteria. The desired area of the image captured is taken as individual columns of pixels. These are fed into LINEDEF column by column as y-position versus intensity. The position of maximum intensity in the line (shown as a peak) is found by fitting order 2 polynomials to the region defined by the user using the y-position of the peak maximum and the half-width of the peak. This enables determination of the peak maximum y-position to better than 0.1 pixel resolution. Using the data from the

previous fit LINEDEF then searches the next image slice, using the previous half-width and y-position data to define the search area within this slice. In this way LINEDEF is able to follow a line of varying thickness very well.

The second part of this work has been to devise a suite of algorithms for analysis of the data obtained from the on-line image capture system using a standard spreadsheet/-curve fitting package with which it is comparatively simple to mathematically manipulate the data and use least squares fitting routines to provide sedimentation coefficient or molecular weight information as required.

For sedimentation velocity we have implemented several methods for analysis: transport (or moving boundary), second moment and radial derivative g(s*) (see Bridgman 1942). The radial derivative for g(s*) was chosen instead of the time derivative (Stafford 1992) as a schlieren image is a radial derivative image ((dn/dr) vs. r) and so this greatly reduces the amount of data processing needed. This does have the disadvantage that it does not remove time independent noise as with the time derivative method. However, this is not critical with the large signal from schlieren optics when solution concentrations of >0.5 mg/ml are employed.

Standard algorithms for non-linear least-squares curve-fitting of concentrations as a function of radial position for sedimentation equilibrium absorption data were adapted for schlieren data to obtain z-average molecular weights and interaction parameters. Algorithms have also been written to extract weight-average molecular weight information from the integral of the dn/dr versus r data, as is done with interferometric and absorption optical systems. Previously manual methods of data capture did not yield sufficient data to apply non-linear least-squares curve-fitting to appropriate mathematical models and consequently the use of the logarithmic plot (Lamm 1929) was mainly used. It was not easy to deduce meaningful results for non-ideal, multi-component and interacting systems from this plot.

It is also possible to apply the approach to equilibrium (Archibald 1947) and the mid-point method (Williams et al. 1958) to obtain weight-average molecular weight data. The former has the advantage that the molecular weight information is obtained rapidly as equilibrium does not need to be attained. The disadvantage of both methods had previously been that an additional synthetic boundary experiment is required to obtain the initial concentration (Klainer and Kegeles 1955). However now differential refractometers of sufficient accuracy are available (in our system a ATAGO DD5, Jencons instrument is used) cross-calibration is therefore possible and simple, without recourse to a synthetic boundary experiment in the ultracentrifuge (Chervenka 1969).

Materials

Sedimentation equilibrium and velocity experiments were performed on the following samples: (a) ovalbumin (Lot No. 14H7035, purchased from Sigma Chemical Co.). The solution was made at 6.98 mg/ml in, and dialysed against, 100 mM PBS buffer, (pH 7.25). (b) dextran (Pharmacia T70, lot 102392), dissolved in 100 mM phosphate chloride buffer (pH 7.0) at 10 mg/ml. (c) apoferritin (Lot No. 97F81455, purchased from Sigma Chemical Co.) dissolved in 100 mM PBS buffer, (pH 7.25) at 10 mg/ml.

Data analysis

Pro Fit (Cherwell Scientific Publishing Ltd., Oxford, UK) was chosen as the curve fitting package as it filled the two mandatory features required for any software used to analyse ultracentrifuge data; it is capable of performing non-linear least-squares curve-fitting and has good publication graphic capabilities (Lewis 1992). *Pro Fit* runs on any Macintosh with system version 7.0 or later. It has a very powerful and simple PASCAL-like syntax for defining mathematical functions and data transformation algorithms. *Pro Fit* can also use externally compiled code hence allowing the possibility of incorporating existing ultracentrifuge analysis programs.

The data captured using the on-line system are presented in the form of three columns, containing a column of run details, radial values (cm) and their corresponding dn/dr values (arbitrary units). The run details column contains the meniscus position, cell base and rotor speed. The user can then apply the appropriate analysis macro. The following macros are described below and examples of their use given.

In all cases the Levenberg-Marquardt algorithm is used for non-linear least-squares curve fitting. All fits are non-weighted, tests with LINEDEF having shown that to an adequate approximation the statistical error in dn/dr estimated was independent of the actual parameter value.

Sedimentation equilibrium

Lamm Plot

This uses Eq. (1) derived by Lamm (1929)

$$d\ln\left(\frac{1}{r}\frac{dn}{dr}\right)\Big/ d(r^2) = M(1-\bar{v}\rho)\omega^2/2RT \qquad (1)$$

when n is the refractive index, r the radial position from the centre of the rotor, ρ is the density of solvent, M the molecular weight, $\bar{v}$ the partial specific volume, ω the angular velocity of the rotor, R the gas constant and T the absolute temperature. A graph of $\ln\left(\frac{1}{r}\frac{dn}{dr}\right)$ versus r^2 has a slope proportional to the z-average molecular weight (M_z). The data for (dn/dr) vs. radius yielded by our system are used to produce such a plot and derive M_z.

Archibald or approach to equilibrium method

The "approach to equilibrium" method first described by Archibald (1947) enables the molecular weight to be calculated from data obtained during the early stages of the run using Eq. (2)

$$M = \frac{RT}{(1-\bar{v}\rho)\omega^2}\frac{(dn/dr)_m}{r_m\, n_m} \tag{2}$$

where the subscript m denotes the value at the solution meniscus.

The value of concentration at the meniscus c_m is obtained from Eq. (3), using cross calibration with a differential refractometer calibrated in centrifuge units to give c_0.

$$c_m = c_0 - \frac{1}{r_m^2}\int_{r_m}^{r_p} r^2 (dn/dr)\, dr \tag{3}$$

where r_p is a radial value within the solution column at which the dn/dr gradient remains at zero.

Sedimentation velocity

Moving boundary method

A plot of $\ln(r_b)$ against $\omega^2 t$ (where r_b is the radial position of the sedimenting boundary and t is time) should give a straight line, the gradient of which is proportional to the sedimentation coefficient. We obtain these data by plotting Gaussian fits to the data set from each image to obtain the peak maximum position. These are then used to derive the sedimentation coefficient using linear regression. An alternative and simpler approach allows the user to select the boundary position.

Second moment method

A theoretically more sound method for determining r_b is to use the second moments of the schlieren gradient curves. Equation (4) is used for the calculation of the radius of the effective migrating boundary at the second moment position (Goldberg 1953)

$$\bar{r}^2 = \frac{\sum_{r_m}^{r_p} r^2 \left(\frac{dn}{dr}\right)}{\sum_{r_m}^{r_p} \left(\frac{dn}{dr}\right)} \tag{4}$$

from which the radius can be derived mathematically.

For a one component system in which there are plateau regions (areas of zero concentration gradient) at both sides of the sedimenting boundary, a plot of $\ln(r_b)$ against $\omega^2 t$ (where r_b is the radial position of the sedimenting boundary, ω is the angular velocity and t is time) should give a straight line where the gradient of the line is the sedimentation coefficient.

g(s*) Method

Apparent sedimentation coefficient distributions can be calculated for a data set using the equation derived by Bridgman (1942). The Bridgman equation (5) for g(s*) derived from (dn/dr) values is

$$g(s^*)_r = (dn(r,t)/dr)\,(\omega^2 rt)\,(r/r_m)^2 \tag{5}$$

The asterisk indicates that in experimental conditions the diffusion coefficient is not equal to zero. Hence the distributions computed using this equation are the apparent distributions. The equation is structured for radial derivative data which is exactly the form of the schlieren image. The apparent value of s* is computed at each position in the boundary using Eq. (6).

$$s^* = \ln(r^*/r_m)/\omega^2 t \tag{6}$$

Various methods of extrapolation of apparent distributions to infinite time to eliminate the effects of diffusion have been developed (Baldwin and Williams 1950, Gralen and Lagermalm 1951, Van Holde and Weischet 1978 and Stafford 1992), but are not as yet implemented by us.

The calculations require the input of time to first image, image interval and number of images. Using data provided by the data capture system, a spreadsheet is computed containing a series of columns of s* versus g(s*) for each set of r versus dn/dr data. A maximum of twenty images can be processed simultaneously. s* versus g(s*) can be plotted and (multiple) Gaussian distributions fitted to obtain the apparent sedimentation coefficient at the maxima. Assuming all species are conserved and the concentration gradient in the plateau is zero, the weight average sedimentation coefficient can also be obtained using the integration shown in Eq. (7)

$$\bar{s}_w = \int_0^\infty s g(s^*)\, ds \tag{7}$$

There remains however the problem of baseline subtraction. Significant redistribution of buffer salts etc. can occur during a sedimentation velocity experiment thus changing the dn/dr profile of solution versus solvent. This must be accounted for to obtain true dn/dr versus radius data for the sedimenting species. One method for this would be the use of double sector cells where one sector contains only solvent. The dn/dr versus radius data for the solvent can then be subtracted from the equivalent data set for the solution. This method is unavailable to us at present as in the region of the solutions near to the meniscus, once solute depletion has occurred, a single line will be produced from both sectors of the cell. This line will diverge at the region of the sedimenting boundary. LINEDEF is unable to deal with this situation at present and will not produce the separate traces of dn/dr. Our current practice is to use the dn/dr from the centre of the solution column as a baseline value, however we are in the process of devising a simple 'background stripping' algorithm which will be implemented when finished.

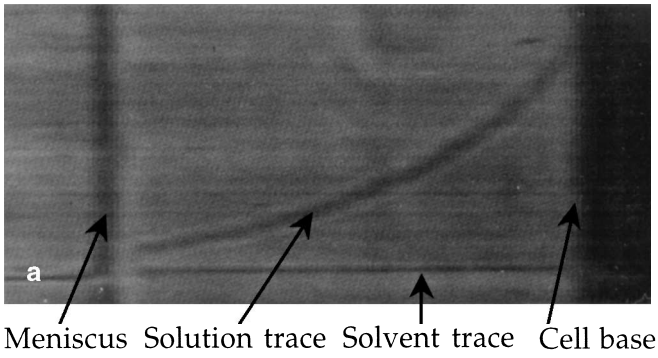

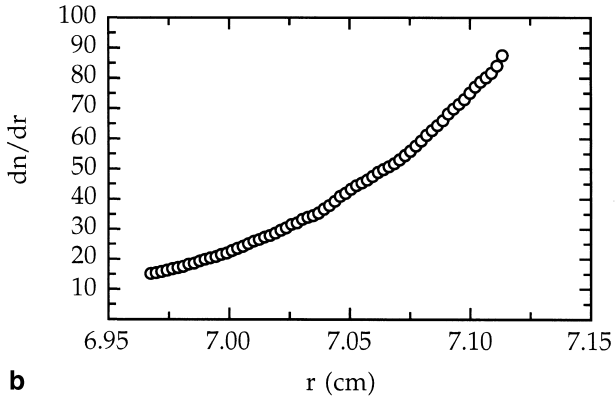

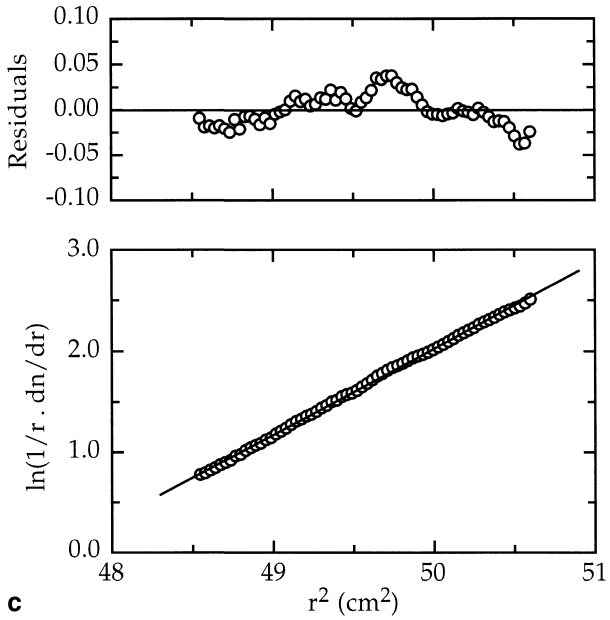

Fig. 1a–c Sedimentation equilibrium experiment with a solution of ovalbumin (6.98 mg/ml in 100 mM PBS buffer, pH 7.25), 20 °C, rotor speed is 19,740 rpm. The figure shows (**a**) the original schlieren image captured after 23 h 36 min, (**b**) dn/dr versus radius produced by LINEDEF, (**c**) a fit of the Lamm equation (–) to experimental data (○) and residuals to the fit

Results

Figure 1 shows the processing of an image from a sedimentation equilibrium experiment with ovalbumin captured using schlieren optics. The native molecular weight of ovalbumin is 45,000 g/mol. The value of M_z obtained from the Lamm equation is 39,700 (SD = 170) g/mol. The apparent molecular weight at the concentration used will be lower than the ideal (formula) mass by an amount which can be computed to a reasonable approximation as the sum of the excluded volume and charge terms. The former has a value of 8 ml/ml for compact spheres, and about the same numerical value (8–9 ml/g) for globular proteins, if we assume their effective swollen partial volume to be in the range 1.3–1.4 ml/g (Squire and Himmel 1979) and the partial specific volume to be around 0.70–0.75 ml/g. To this must be added the charge term, which for ovalbumin in 100 mM neutral salt, with a net charge equal to –9 to –16 (see Tanford 1963), will be in the region 6–15 ml/g (calculated from standard relationships). We may thus take the sum value for BM, where B is the second order virial coefficient as defined for sedimentation equilibrium (= 2B if defined in osmotic pressure terms), as having a value in the range 14–24 ml/g, (mean 19.5 ml/g). For a protein concentration of 0.00698 g/ml, the apparent molecular mass is then predicted to be $45{,}000/(1 + 0.00698 * 19.5) = 39{,}612$ g/mol. Given the residual uncertainty in the precise value for BM, the uncertainties in degree of glycosylation and surface charge, and the fact that the average produced by the Lamm plot is derived from a captured data set which may not be precisely symmetrical around the point of conservation of the initial solute concentration, the experimentally obtained value is in very good agreement with this. The clear downward curvature of the plot (as seen in the residuals) is visually indicative of this 'non-ideality' of the system.

Figure 2 shows an approach-to-equilibrium experiment with dextran, together with the meniscus extrapolation. From these data we have $c_o = 0.137$, $c_m = 5.630 \times 10^{-3}$ and Mw = 22,200 g/mol. Again this result is in the range expected for such a polydisperse sample as dextran under these experimental conditions.

Figure 3 shows a sedimentation velocity experiment with apoferritin. In addition to the monomer, the presence of a small amount of dimeric protein can be seen in this experiment. The results from $g(s^*)_{(max)}$ give s = 16.537 (±0.006) S for the trailing (left-hand) peak and s = 23.839 (±0.054) S for the leading (right hand) peak. These results compare favorable to those obtained by the moving boundary method (15.91 ± (0.13) S and 23.64 (± 0.23) S respectively).

Discussion

As can be seen above the data from our image processing package yield accurate representations of the original images and can provide data of much higher resolution than

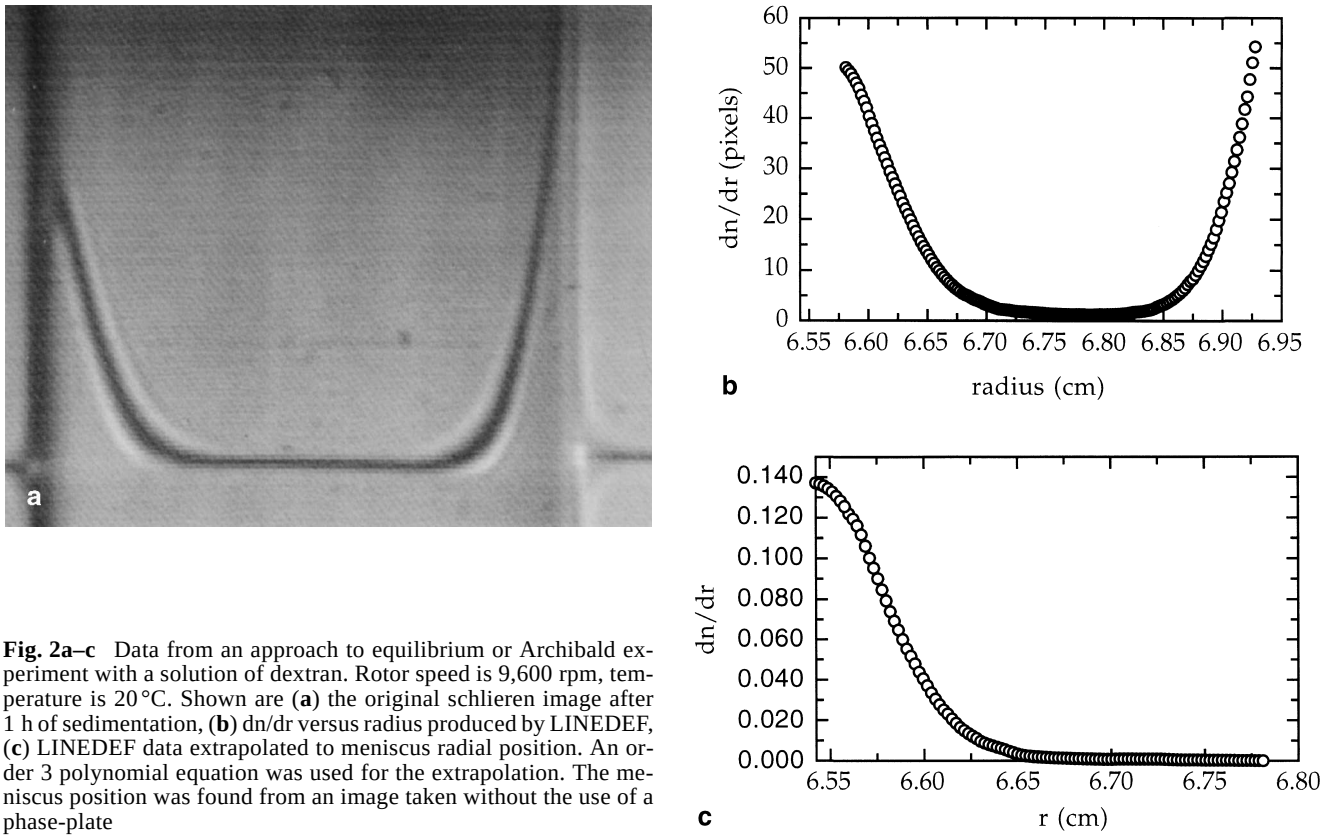

Fig. 2a–c Data from an approach to equilibrium or Archibald experiment with a solution of dextran. Rotor speed is 9,600 rpm, temperature is 20 °C. Shown are (**a**) the original schlieren image after 1 h of sedimentation, (**b**) dn/dr versus radius produced by LINEDEF, (**c**) LINEDEF data extrapolated to meniscus radial position. An order 3 polynomial equation was used for the extrapolation. The meniscus position was found from an image taken without the use of a phase-plate

was possible previously with microcomparator methods, and in a much reduced time. This has enabled us to use a greater variety of analysis methods and hence much more information can now be gained from the use of schlieren optics.

The mathematical manipulations described above are shown to give greater precision than has previously been easily possible (between 0.1 and 0.02% of s^*_{max}) and give results which are in very good agreement, both with each other and with those expected from literature or independent experimentation (Clewlow, unpublished data). The accuracy of the results however, cannot be as good as this precision, due to uncertainties in rotor temperature and other factors which are beyond accurate measurement at present.

This methodology has removed many of the problems which have reduced the popularity of schlieren optical systems on analytical ultracentrifuges. The imaging system can be adapted to fit almost any analytical ultracentrifuge and can be also used with absorption and interference optics, and the computer software used runs stable, efficient algorithms.

Schlieren optics have several advantages over systems more commonly used with the AUC: absorption optics are of inherently limited precision for defining solute distributions in the AUC. The 'noise' is of the order of 1% at best in a single reading of extinction at a given radial position. The Beer-Lambert law also limits the use of absorption optics to relatively dilute solutions where the solute has a useable chromophore. Refractometric optics, which detect the optical path difference arising from the presence of solute, need no chromophore and can achieve a precision an order of magnitude better than absorption optics (1/300th of a Rayleight fringe in a total increment of 3 fringes is feasible).

Of the two types of refractometric optics used in the AUC, namely Rayleigh interferometric and differential refractometric (schlieren), the former have normally been considered to be of much the higher precision (see for example the monograph by Lloyd (1974) and the earlier papers by Svensson (1954) and others quoted therein). Schlieren optics have been seen as useful only for work with higher concentrations of solute, especially for sedimentation velocity studies on such systems, where the differential form of the data (i.e. dn/dr vs. r) makes simple interpretations easier, and where window distortion has, unlike in the case of interference optics, negligible effects on the patterns observed.

This view has recently been challenged. Rowe et al. (1989) have pointed out that a simple relationship can be derived which connects the Fresnel fringe spacings observed in schlieren optics using a phase plate diaphragm with the interferometric fringe shifts observed in Rayleigh optics. This relationship involves a two-fold integration (schlieren data to Rayleigh data), or a two-fold differentiation for the reverse transformation. Noise in the basic sig-

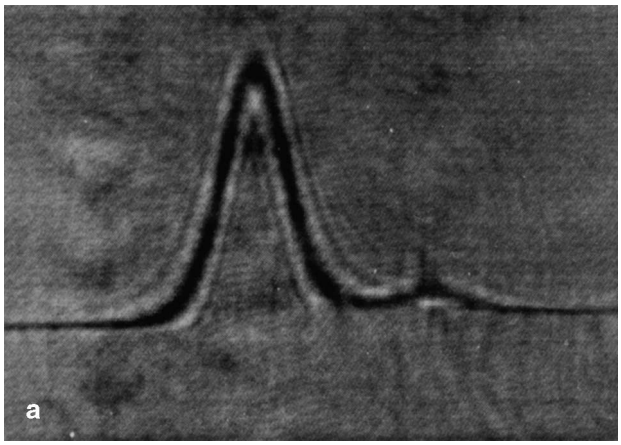

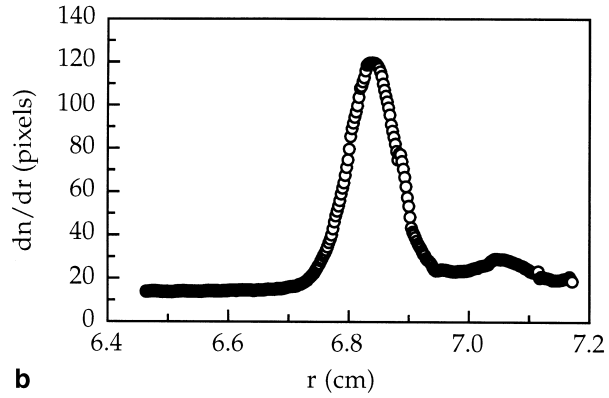

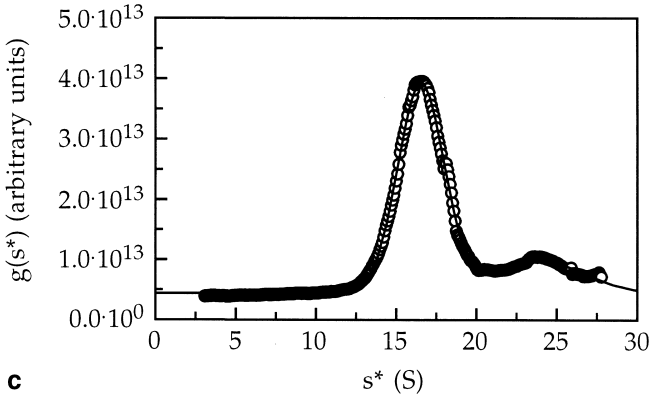

Fig. 3a–c Sedimentation velocity experiment with apoferritin, rotor speed is 34,720 rpm temperature is 20 °C. Shown are (**a**) the original schlieren image captured after 61 minutes of sedimentation, (**b**) dn/dr versus radius produced by LINEDEF and (**c**) apparent g(s*) versus apparent sedimentation coefficient

nal is well known in all numerical work to be much reduced/increased respectively by these procedures. Simple computer simulation (Rowe, unpublished) shows that for data sets of the relevant size an improvement in signal/noise ratio of around 10-fold is expected from a two-fold numerical integration procedure. Thus assuming that the noise in the Fresnel pattern signal formed from schlieren optics is no worse than an order of magnitude greater than the noise in the Rayleigh fringe signal, which is the case, we can assert that the precision attainable in the quantity Δn (difference in refractive index between two radial positions) must be closely comparable in the two cases, though not necessarily identical. In principle, therefore, a suitable algorithm for the analysis of a Fresnel fringe pattern of the type yielded by schlieren optics should yield an estimate for the zeroth order (denoting the value of the dn/dr) which after integration will yield an estimate for the refraction increment at any radial position which will be of a precision comparable to that provided by interferometric optics. A software set based upon these principles has been written by us (Fresnel Workbench). Unfortunately it transpires that the scans across a schlieren pattern produced by a phase plate incorporating, as is normal, a thin wire of evaporated metal are only a poor approximation to a true Fresnel function. Probably the compound nature of the diaphragm is responsible for this fact. Under these circumstances the precision obtained in estimating the coordinates of the zeroth order fringe was found to be unacceptably low, being little if at all better than that given by manual methods. The simpler, but very stable, LINEDEF procedure described above yields a precision which, if translated into Rayleigh fringe terms, is estimated to be equivalent to better than f/50. Where high concentrations (10–100+ fringes) are being used, which is a major point of the whole methodology, the percentage precision is thus high, and comparable to good practice automated interference work conducted at the usual concentration levels.

Thus it is our conclusion that schlieren optical systems are of significant value to studies with the AUC and that our analysis package can greatly simplify the analysis from these systems whilst increasing precision and data analysis options.

Acknowledgements The authors would like to acknowledge the invaluable assistance of Mr. Dipak Patel with computer programming in this work. The NCMH is funded by the BBSRC and EPSRC.

References

Archibald WJ (1947) A demonstration of some new methods of determining molecular weights from the data of the ultracentrifuge. J Phys Colloid Chem 51:1204–1211

Baldwin RL, Williams JW (1950) Boundary spreading in sedimentation velocity experiments. J Am Chem Soc 72:4325–4327

Bridgman WB (1942) Some physical chemical properties of glycogen. J Am Chem Soc 64:2349–2350

Chervenka CH (1969) A manual of methods for the analytical ultracentrifuge. Spinco Division, Beckman Instruments, Palo Alto

Goldberg RJ (1953) Sedimentation in the ultracentrifuge. J Phys Chem 57:194–202

Gralén N, Lagermalm G (1951) A contribution to the knowledge of some physico-chemical properties of polystyrene. J Phys Chem 56:514–515

Klainer SM, Kegeles G (1955) Simultaneous determination of molecular weights and sedimentation constants. J Phys Chem 59: 592–593

Lamm O (1929) Zur Theorie und Methodik der Ultrazentrifugierung. Z Physik Chem (Leipzig) A143:177–182

Lewis MS (1992) Data acquisition and analysis systems for the absorption optical system of the analytical ultracentrifuge. In: Harding SE, Rowe AJ, Horton JC (eds) Analytical ultracentrifugation in biochemistry and polymer science. Royal Society of Chemistry, London, pp 126–137

Lloyd PH (1974) In: Optical methods in ultracentrifugation, electrophoresis and diffusion (Monographs on Physical Biochemistry series). Clarendon Press, Oxford, Chapter 3, pp 21–37

Rowe AJ, Wyne-Jones S, Thomas D, Harding SE (1989) Analysis of solute concentration and concentration derivative distributions by means of frameshift Fourier and other algorithms applied to Rayleigh interferometric and Fresnel fringe patterns. Fringe analysis, GT Reid (ed). Proc SPIE 1163:138–148

Schachman HK (1959) Ultracentrifugation in biochemistry. Academic Press, New York

Squire PG, Himmel M (1979) Hydrodynamics and protein hydration. Arch Biochem Biophys 196:165–177

Stafford WF III (1992) Boundary analysis in sedimentation transport experiments: a procedure for obtaining sedimentation coefficient distributions using the time derivative of the concentration profile. Anal Biochem 203:295–301

Svensson H (1954) The second order aberrations in the interferometric measurement of concentration gradients. Optica Acta 1:25–32

Tanford C (1963) Physical chemistry of macromolecules. John Wiley, New York, pp 427

Van Holde KE, Weischet WO (1978) Boundary analysis of sedimentation velocity experiments with monodisperse and paucidisperse solutions. Biopolymers 17:1387–1403

Williams JW, Van Holde KE, Baldwin RL, Fujita H (1958) The theory of sedimentation analysis. Chem Revs 58:715–723